Journal of Photochemistry & Photobiology, B: Biology 240 (2023) 112654

Contents lists available at ScienceDirect

Journal of Photochemistry & Photobiology, B: Biology

journal homepage: www.elsevier.com/locate/jphotobiol

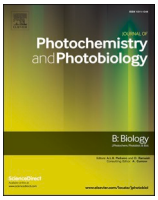

Long-term blue light exposure impairs mitochondrial dynamics in the retina in light-induced retinal degeneration in vivo and in vitro

Liyin Wang [a,b,1], Xin Yu [a,b,1], Dongyan Zhang [c,1], Yingying Wen [a,b], Liyue Zhang [a,b], Yutong Xia [a,b], Jinbo Chen [a,b], Chen Xie [a,b], Hong Zhu [a,b], Jianping Tong [a,b,*], Ye Shen [a,b,*]

[a] Department of Ophthalmology, First Affiliated Hospital, College of Medicine, Zhejiang University, Hangzhou, Zhejiang 311003, China
[b] Clinical Research Center, First Affiliated Hospital, College of Medicine, Zhejiang University, Hangzhou, Zhejiang 311003, China
[c] Department of Ophthalmology, Shaoxing Central Hospital, Shaoxing 312030, Zhejiang, China

ARTICLE INFO

Keywords:
Dry age-related macular degeneration
RPE cells
Blue light
Oxidative stress
Mitochondrial dynamics

ABSTRACT

Long-term light exposure, especially in the spectrum of blue light, frequently causes excessive oxidative stress in dry age-related macular degeneration (AMD). Here, to gain insight into the underlying mechanism, we focused on mitochondrial dynamics alterations under long-term exposure to blue light in mouse and retinal cells. Six-month-old C57BL/6 mice were exposed to blue light (450 nm, 800 lx) for 2 weeks. The phenotypic changes in the retina were assayed using haematoxylin-eosin staining and transmission electron microscopy. Long-term blue light exposure significantly thinned each retinal layer in mice, induced retinal apoptosis and impaired retinal mitochondria. A retinal pigment epithelial cell line (ARPE-19) was used to verify the phototoxicity of blue light. Flow cytometry, immunofluorescence and MitoSox Red probe experiments confirmed that more total and mitochondria-specific ROS were generated in the blue light group than in the control group. Mito-Tracker Green probe showed fragmented mitochondrial morphology. The western blotting results indicated a significant increase in DRP1, OMA1, and BAX and a decrease in OPA1 and Bcl-2. In conclusion, long-term exposure to blue light damaged the retinas of mice, especially the ONL and RPE cells. There was destruction and dysfunction of mitochondria in RPE cells in vivo and in vitro. Mitochondrial dynamics were disrupted with characteristics of fusion-related obstruction after blue-light irradiation.

1. Introduction

Age-related macular degeneration (AMD) is considered as the most common cause of blindness in developed countries [1,2], and its prevalence is predicted to increase to 288 million worldwide by 2040 [3]. Late-stage AMD is divided into wet AMD and dry AMD according to whether neovascularization occurs [4], and anti-VEGF therapy has recently been suggested to be a viable treatment for wet AMD [5,6]. However, there is still no effective therapy for dry AMD. Previous studies have revealed that the mechanism of dry AMD is based on dysfunction of the retinal pigment epithelium (RPE), which is required to maintain photoreceptor (PR) survival, renewal and normal function [7].

The RPE, a monolayer of pigment cells, is situated between the neural retina and choroid and performs vital functions such as formation of the outer blood–retinal barrier, transepithelial transport, maintenance of the retinoid cycle, phagocytosis, degradation of photoreceptor outer segment tips, and protection against light and oxidative stress [8]. Since RPE impairment contributes remarkably to AMD [9], it is imperative to identify the mechanisms behind RPE degeneration to investigate the pathogenesis of dry AMD.

With the wide adoption of light-emitting diode (LED) lamps, the hazard to eyes from this artificial light source has gradually attracted attention. Ultraviolet (UV) rays shorter than 300 nm and most UV rays between 300 nm and 400 nm are prevented from reaching the retina via the cornea and crystalline lens, respectively, and thus the short wavelength light that can reach the retina is mainly in the 400–500 nm range [10]. The International Commission on Non-Ionizing Radiation Protection (ICNIRP) has proposed a guideline: 110 kJ/m^2 has been evaluated as the toxic dose of blue light from ocular instruments that induces macroscopically observable retinal lesions [11,12]. An increasing number of studies has revealed that long-term blue light (400–500 nm) exposure induces oxidative stress in the retina and causes severe damage

* Corresponding authors at: Department of Ophthalmology, First Affiliated Hospital, College of Medicine, Zhejiang University, Hangzhou, Zhejiang 310003, China.
E-mail addresses: tongjp2000@hotmail.com (J. Tong), idrshen@zju.edu.cn (Y. Shen).
[1] Contributed equally.

https://doi.org/10.1016/j.jphotobiol.2023.112654
Received 18 July 2022; Received in revised form 9 January 2023; Accepted 21 January 2023
Available online 24 January 2023

to retinal tissues, especially RPE cells [13,14], with harmful effects peaking at 440 nm [15,16]. Due to the intense metabolic activity and high oxygen consumption in the retina, the RPE is vulnerable to oxidative damage that causes pathological changes related to AMD [8]. Thus, a clear understanding of the mechanism underlying the effect of blue light-induced oxidative stress in RPE cells and subsequent RPE degeneration is the key to preventing retinal damage.

Mitochondria are crucial organelles that produce reactive oxygen species (ROS) in cells [17,18]. Excessive oxidative stress leads to the overproduction of ROS and impaired oxidative phosphorylation in mitochondria, resulting in further mitochondrial ROS production and leading to a vicious cycle involving mitochondria, ROS and AMD development [19]. Mitochondria are dynamic organelles that undergo continuous fission and fusion to maintain their normal structure and functions and subsequently maintain ROS levels within the normal range [20]. Mitochondrial fusion events promote the exchange of substances among mitochondria through the formation of long, large mitochondrial networks and help maintain biogenetic activity [21]. In contrast, fission events result in short, small or fragmented mitochondria and facilitate the engulfment of irreversibly damaged mitochondria via autophagy [22]. An imbalance of fusion/fission dynamics is the key to the formation of the vicious cycle between ROS overproduction and mitochondrial dysfunction. However, researchers have not yet clearly determined whether long-term blue light exposure induces retinal degeneration by impairing mitochondrial dynamics in retinal cells. To the best of our knowledge, alterations in mitochondrial dynamics have not been analysed in vivo. Therefore, this study was performed with the aim of first exploring this mechanism using pigmented mice and in vitro models.

Here, we exposed six-month-old C57BL/6 mice to blue LED lamps (450 ± 15 nm, 800 lx) to cause retinal degenerative changes. We found that retinal tissues were significantly damaged by long-term blue light exposure based on histological haematoxylin–eosin (HE) staining and terminal deoxynucleotidyl transferase dUTP nick end labelling (TUNEL). Destruction of mitochondria in the RPE layer was observed in the blue light group using transmission electron microscopy, and the expression levels of mitochondrial dynamics-related proteins were analysed using western blotting and immunohistochemistry. As expected, the fission-related proteins DRP1 and OMA1 were upregulated, but the fusion-related protein OPA1 was obviously downregulated. We used a widely accepted light-induced retinal degeneration model with ARPE-19 cells in vitro to further investigate the underlying mitochondrial changes. Ultimately, we indicate that mitochondrial dynamics were disrupted with characteristics of fusion-related obstruction after blue light irradiation.

2. Materials and Methods

2.1. Animals and Blue Light Damage Models

Due to the impossibility of exposing humans to monochromatic light, six-month-old female C57BL/6 mice employed in this research were obtained from the laboratory of Zhejiang Academy of Medical Sciences. The animals were randomly assigned to two groups of seven as the negative control group and blue light group. All animals were supplied with continuous food and water in 12-h periods of dark and light (on at 8 AM and off at 8 PM) and 22 °C environment. Different from the control group, the specific LED light tubes (peak value 450 nm, half bandwidth 15 nm) were customized for the blue light group. The intensity of the illumination was set up at 800 lx and detected by a luminometer (HOPOOCOLOR OHSP350C, China). Two weeks of exposure with the irradiance in our setup corresponded to the toxic energy threshold evaluated by ICNIRP. After two weeks of illumination, the light-damage models were built, and all animals were killed with dislocation of the cervical vertebra for further study. All experimental procedures conformed to the ARVO Statement for the Use of Animals in Ophthalmic and Vision Research. This research was ratified by the Tab of Animal Experimental Ethics Inspection of the First Affiliated Hospital, Zhejiang University School of Medicine.

2.2. Histopathological Examination

At the endpoint of two weeks of illumination, the eyeballs of mice from each group were quickly enucleated after cervical dislocation, and histological slides (thickness: 3 μm) were prepared in a routine manner. After staining with haematoxylin-eosin (HE), the slides were observed with a light microscope (Olympus Co., Tokyo, Japan). Thickness of the retina and other parts of globes was measured at three same regions (left, middle, and right sides) in each image using KFBIO Digital Slide Viewer software (Konfoong Biotech International Co., Ltd.; Zhejiang, China) and was recorded as the mean ± SD.

In addition, TUNEL (terminal deoxynucleotidyl transferase dUTP nick end labelling) staining (One Step TUNEL Apoptosis Assay Kit C1088, Beyotime; Shanghai, China), a common and intuitive way to label apoptosis, was performed to detect the apoptosis level in the retina. According to the protocol, after successively dewaxing in xylene, 100% ethanol, 90% ethanol, 70% ethanol and distilled water, the histological sections were washed three times in phosphate-buffered saline (PBS; pH 7.4) at room temperature. Drops of 20 μg/mL DNase-free protease K were applied to the samples for 25 min at room temperature to enhance the combination of the probe, and then the slides were rinsed in PBS repeatedly as above. Afterwards, each sample was incubated with 50 μL TUNEL test solution mixed with 5 μL terminal deoxyribonucleotidyl transferase (TdT) enzyme and 45 μL fluorescent labelling solution in the dark at 37 °C for 1 h and purged in PBS solution three times. After sealing with anti-fluorescence quenching sealing solution, the film was observed under an ortho fluorescence microscope (BX53, Olympus Co.; Tokyo, Japan).

Then, immunohistochemistry was used to intuitively reveal the protein expression distribution in the retina. Sections were split and blocked in 5% bovine serum albumin dissolved in PBS and incubated with OMA1 antibody (sc-515788; Santa Cruz Biotechnology; 1:50) at 4 °C overnight and then conjugated with secondary antibody for 1 h. Afterwards, the tissue specimens were dyed with 3,3-diaminobenzidine (DAB) substrates and further dewatered. Observed under a light microscope, the relative expression level of OMA1 was analysed by Image J software.

2.3. Transmission electron Microscopy

After enucleation from the mouse orbital cavity and clearing of the vitreous, lens and surrounding connective tissue, the posterior sclera and retina near the optic nerve were cut into 2 mm × 1 mm strips, immediately saturated with electron microscope fixing solution (Wuhan Servicebio; Wuhan, China) at 4 °C for 24 h and then rinsed in PBS for 15 min three times. After being fixed with 1% osmic acid reagent for 1 h and washed three times in PBS, the sections were gradually dehydrated by 30%, 50%, 70%, and 80% ethanol solutions, and each treatment lasted for 10 min. Afterwards, the samples were successively shifted into 90% and 95% acetone solutions followed by pure acetone for 20 min. After dehydration, samples were gradiently treated with a mixture of different proportions of Spurr embedding agent and acetone, ultimately with pure Spurr overnight at room temperature. The sections were sliced into serial ultrathin sections and stained with uranyl acetate and lead citrate. The ultrastructural features and mitochondrial changes were observed under a Tecnai G2 spirit 120 kV transmission electron microscope (FEI; USA).

2.4. ARPE-19 Culture and Experimental Treatment

ARPE-19 cells within passages 2–20 were used in this study and acquired from Hunan Fenghui Biotechnology Co., Ltd., China. All

cultures were maintained at 37 °C in 5% CO2 and a humidified atmosphere. Cells were incubated on T25 flasks in Dulbecco's modified Eagle's medium/F-12 nutrient medium (CR12400-S, Cienry Biotechnology; Zhejiang, China) supplemented with 10% heat-inactivated foetal bovine serum (10099–141, Gibco BRL; MD, USA). Cells were passaged when they reached 90% confluence through trypsinization with 0.25% trypsin-EDTA (25200–056, Gibco BRL; MD, USA) and seeded into suitable culture plates for the next experiments.

The blue light damage models in vitro were set up by exposing to customized LED tubes as mentioned above. The illuminance towards ARPE-19 was controlled at 2.3 mW/cm2. In the meantime, the positive control group was treated with tert-butyl hydroperoxide (TBHP) (458139, Sigma–Aldrich; MO, USA) in the dark when reaching 50% confluence to interpret the oxidative stress of blue light exposure.

2.5. Protein Extraction and Western Blot

After separation from the eyeball, mouse retina tissue was immediately transferred into 2 mL microcentrifuge tubes on ice and immersed in 100 μL RIPA buffer (89900, Thermo Fisher Scientific; MA, USA) containing 1% PMSF, 1% phosphatase inhibitors and 1% protease inhibitor (HY-K0022, HY-K0010, MedChemExpress; NJ, USA). The tissue was added to 4 small grinding media and ground at 60 Hz for 3 min twice in Cryogenic Grinder (JXFSTPRP-CL, Jingxin Industrial Development Co., Ltd.; Shanghai, China). After centrifugation (12,000 ×*g*, 15 min, 4 °C), the protein concentration was determined using a BCA Protein Assay Kit (P0011, Beyotime; Shanghai, China) and quantified with RIPA solution and 5× SDS–PAGE Sample Loading Buffer (BL502B, Biosharp Life Science; China) at 100 °C for 10 min to mix them thoroughly.

ARPE-19 cells treated with stimulation in 6-well plates were trypsinized with 0.25% trypsin-EDTA for 2 min and centrifuged (1000 rpm, 4 min, room temperature) to precipitate the cells. After washing in PBS once, the cells were resuspended in 50 μL RIPA mixture as mentioned above and incubated for 15 min at 4 °C. Furthermore, cell specimens were centrifuged and tested by a BCA Protein Assay Kit and finally quantified in the same way as mouse protein samples.

Total mouse or cell protein lysates (30 μg) were loaded onto GenScript SurePAGE Bis-Tris 4–20% gels (M00657, GenScript; NJ, USA) for electrophoresis and subsequently transferred onto 0.45 μm PVDF membranes using 1× transfer buffer (L00726C, GenScript; NJ, USA). Membranes were soaked in 5% skim milk (232100, BD Pharmingen; CA, USA) in 1× TBST (BL608A, Biosharp Life Science; China) for two hours at room temperature, followed by incubation with the appropriate primary antibody overnight at 4 °C and sequential secondary antibodies the next day according to standard protocols. Proteins were assessed using enhanced chemiluminescence (ECL) western blotting detection reagents (BL523B, Biosharp Life Science; China), and pictures were acquired by a gel imaging acquisition and analysis system (GenoSens 2000, Clinx Science Instrument Co., Ltd.; Shanghai, China). The antibodies used in western blotting were as follows: anti-GAPDH (5174S; Cell Signaling Technology; 1:5000); anti-OPA1 (27733–1-AP; Proteintech; 1:3000); anti-DRP1 (sc-271583; Santa Cruz Biotechnology; 1:500); anti-OMA1 (sc-515788; Santa Cruz Biotechnology; 1:500); anti-Bax (D2E11; Cell Signaling Technology; 1:1000); anti-Bcl-2 (AF6139; Affinity Biosciences; 1:500); anti-rabbit IgG, HRP-linked antibody (7074P2; Cell Signaling Technology; 1:5000); and anti-mouse IgG, HRP-linked antibody (A21010; Abbkine Scientific; 1:10000).

2.6. Cell Viability

To evaluate the effect of blue light on cell proliferation, ARPE-19 cells were seeded into 96-well plates, and each well contained 1×10^4 cells/100 μL complete culture medium. After 24 h, the media was replaced with 100 μL of fresh complete media containing different concentrations of TBHP, in which groups with blank media accepted blue light. Twelve hours later, the supernatant of the cell cultures was exchanged with 100 μL serum-free media including 10% CCK-8 labelling reagent (BS350, Biosharp Life Science; China). At the end of treatment at 37 °C for 1 h, the absorbance of the mixture at 450 nm was measured by a SpectraMax i3x multiwavelength measurement system (Molecular Devices; CA, USA). The scale of the mean optical densities (ODs) of the experimental specimen and that of the control illustrated the cell viability.

2.7. Immunofluorescence

ARPE-19 cells were seeded on the top surface of glass cover slips in 24-well plates and fixed in 4% paraformaldehyde for 30 min. The cells were permeabilized in PBS containing 0.2% Triton-X reagent for 10 min at room temperature and blocked with 3% bovine serum albumin in PBS for 30 min. The cells were incubated with an OMA1 antibody (sc-515788; Santa Cruz Biotechnology; 1:100) diluted in 1% bovine serum albumin solution overnight at 4 °C with Alexa Fluor anti-rabbit 596 (111–585-003; Jackson ImmunoResearch Laboratories, Inc.; PA, USA) as a secondary antibody the following day. The sections were fixed with mounting medium with DAPI (ab104139, Abcam; MA, USA) containing 4′,6-diamidino-2-phenylindole (DAPI). The images were captured using an ortho fluorescence microscope, and quantitative analysis of OMA1 relative fluorescence intensity was performed using Image J software.

2.8. Reactive Oxygen Species (ROS) Detection

General ROS production was quantified/detected by flow cytometry and immunofluorescence. Flow cytometry was performed using CM-H2DCFDA Reactive Oxygen Species (ROS) Detection Reagents (C6827, Invitrogen, CA, USA). A stock solution of 1 mM was prepared by adding 86.5 μL of dimethylsulfoxide (DMSO) (196055, MP Biomedicals, LLC; CA, USA) to a vial containing 50 μg CM-H2DCFDA. Then, a working solution of 10 μM CM-H2DCFDA was made by dissolving 1 μL of this stock solution in 1 mL of serum-free culture media. At the end of treatment, the original media was replaced by working solution and treated for 30 min at 37 °C. The results were measured using a CytoFLEX LX flow cytometer (Beckman Coulter, Miami, USA).

Immunofluorescence of ROS production was detected using a Reactive Oxygen Species Detection kit (S0033S, Beyotime, Shanghai, China). A concentration of 10 μM FITC-labelled DCFH-DA probe diluted in serum-free culture media was added and incubated for 20 min at 37 °C after discarding the cell supernatant. Cells were rinsed in PBS three times to fully remove uncombined DCFH-DA and detected under an inverted fluorescence microscope (IX73, Olympus Co., Tokyo, Japan).

2.9. MitoSox Red Labelling in ARPE Cells

MitoSox Red was gained from Yeasen Biotechnology (40778ES; Shanghai, China), a probe specifically targeting mitochondria, to selectively detect hyperoxide produced by mitochondria and used pursuant to procedures previously described [23]. ARPE-19 cells were seeded in special confocal dishes (BS-20-GJM, Biosharp Life Science; China). After treatments, cells were loaded with 5 μM MitoSox Red diluted in HBSS for 10 min at 37 °C after washing in preheated HBSS three times. After washing in HBSS three times again, codyeing with Hoechst (33342, Beyotime; Shanghai, China; 1:5000) was performed at room temperature for 10 min. The intensity of fluorescence was observed under a confocal fluorescence microscope (FV1000, Olympus Co., Tokyo, Japan) and analysed using Image J software.

2.10. Apoptosis Assay

Assessment of apoptosis was performed with flow cytometry using an Annexin V-FITC Apoptosis Detection Kit (BMS500FI, Thermo Fisher Scientific; MA, USA) according to the manufacturer's protocols. ARPE-

19 cells were seeded into 6-well plates, and experimental wells were treated with 100 μM TBHP or blue light for 12 h. The cells were trypsinized, centrifuged in PBS twice and resuspended in 200 μL 1× buffer made by mixing 4× buffer and ddH_2O. Then, the cells were costained using 10 μL propidium iodide and 5 μL Annexin V-FITC reaction reagent in testing tubes at room temperature for 15 min in the dark and analysed using a CytoFLEX LX flow cytometer.

2.11. Assessment of Mitochondrial Morphology

The Mito-Tracker Green probe was obtained from Beyotime Biotechnology (C1048; Shanghai, China). ARPE-19 cells were seeded in confocal dishes. After treatments, cells were loaded with 100 nM Mito-Tracker Green probe for 15 min at 37 °C after three washes with pre-heated HBSS. After three addition washes with HBSS, costaining with Hoechst was performed at room temperature for 10 min. The morphology of mitochondria was observed under a confocal fluorescence microscope and analysed using Image J software.

2.12. Statistical Analysis

Experiments in this study were performed in triplicate and repeated at least three times. Data are presented as the means ± SDs. To estimate whether the differences between the investigated groups were mutually significant, IBM SPSS Statistics, a highly recognized software, was used to perform one-way analysis of variance (ANOVA) and *t*-tests. A probability value of $P < 0.05$ indicated a statistically significant difference.

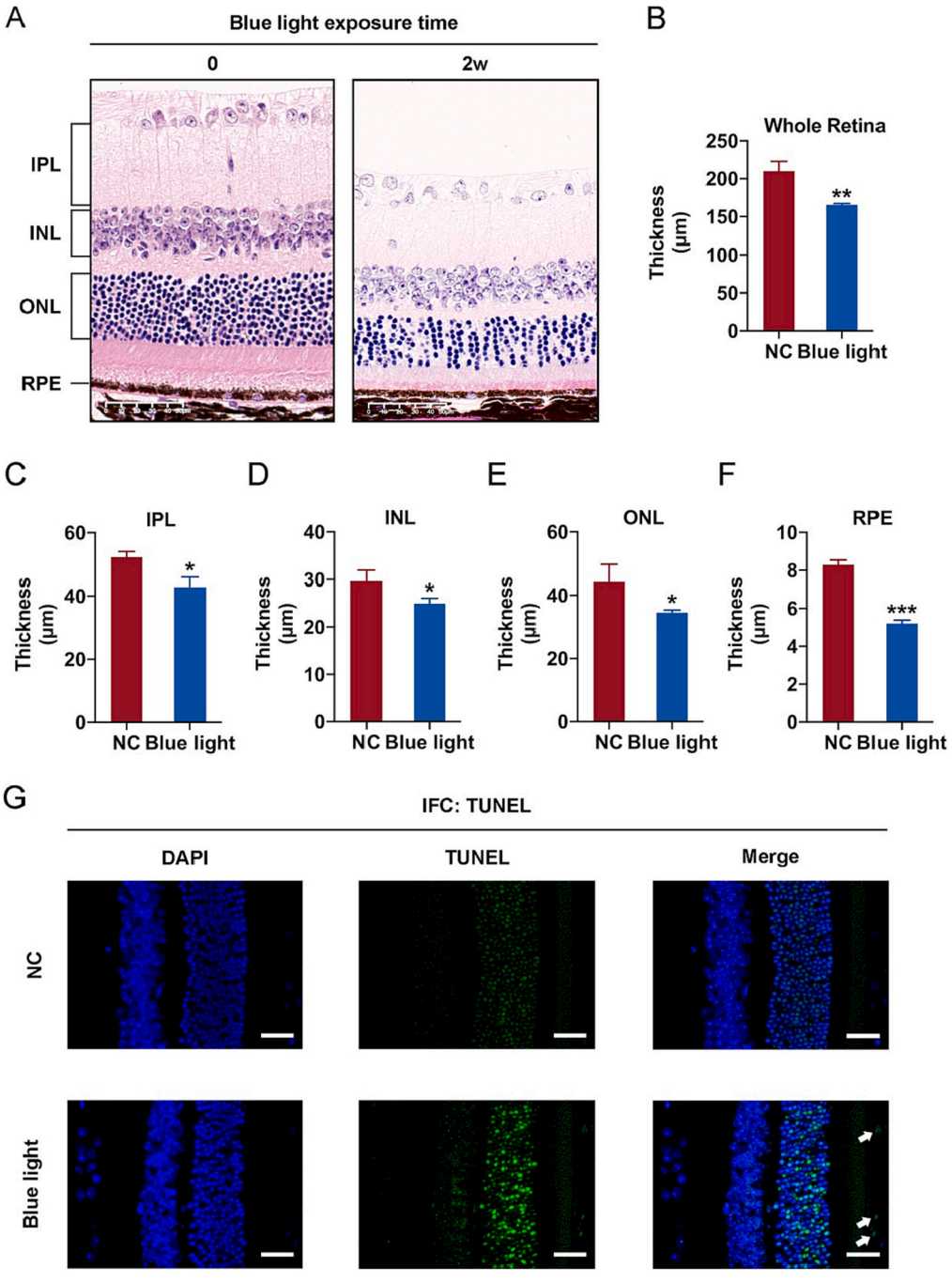

Fig. 1. Effects of long-term blue light exposure on the retina in C57BL/6 mice. (A) A group exposed to blue light for 2 weeks was compared with a negative control group. HE staining determined the position of each layer of the retina, including the inner plexiform layer (IPL), inner nuclear layer (INL), outer nuclear layer (ONL) and retinal pigment epithelium (RPE) layer. The thicknesses of (B) the total retina, (C) IPL, (D) INL, (E) ONL, and (F) RPE layer were quantitatively measured to represent the retinal status (* $p < 0.05$, ** $p < 0.01$, *** $p < 0.001$). (G) TUNEL immunostaining was performed to assay the levels of apoptosis in retinal sections. Arrows indicated apoptotic cells in RPE layer. Blue: nuclei stained with DAPI, green: TUNEL-positive cells. Scale bar = 200 μm. (For interpretation of the references to colour in this figure legend, the reader is referred to the web version of this article.)

3. Results

3.1. Severe Damage to Mouse Retinal Tissues Caused by Exposure to Blue Light

Through the establishment of a mouse blue light-induced damage model (illuminance: 800 lx) and retinal histological analysis, we found that long-term exposure to blue light had a certain damaging effect on retinal tissue. As shown in Fig. 1A, HE-stained sections depicted the layer distribution of retinal tissue: the inner plexiform layer (IPL), inner nuclear layer (INL), outer nuclear layer (ONL) and retinal pigment epithelium (RPE) layer were observed. Through repeated measurement using KFBIO Digital Slide Viewer software and statistical analysis of the thickness of each layer with specific analysis software, we found that blue light exposure for 2 weeks significantly reduced the thickness of the total retina and of each layer of retinal tissue compared to that in the negative control group (Fig. 1B-F). The thicknesses in the control group were as follows: 210.09 ± 12.78 μm in the whole retina, 52.32 ± 1.77 μm in the IPL, 29.64 ± 2.33 μm in the INL, 44.21 ± 5.58 μm in the ONL, and 8.30 ± 0.25 μm in the RPE. The thicknesses in the experimental group were as follows: 165.56 ± 1.71 μm for the whole retina, 42.89 ± 3.13 μm for the IPL, 25.00 ± 1.04 μm for the INL, 34.57 ± 0.81 μm for the ONL, and 5.21 ± 0.17 μm for the RPE. Furthermore, we performed a TUNEL immunofluorescence assay to evaluate apoptosis in the retina, and representative images revealed apoptotic cells (green) in the ONL (Fig. 1G). There were more apoptotic cells in RPE of blue light group as arrows indicated. Long-term exposure of mouse retinas to blue light thinned each retinal layer and caused apoptosis, especially in the ONL and RPE.

3.2. Mitochondrial Morphological Alteration and Dynamic Marker Changes in Mice Exposed to Blue Light

Mitochondrial homeostasis is considered vital for cell metabolism

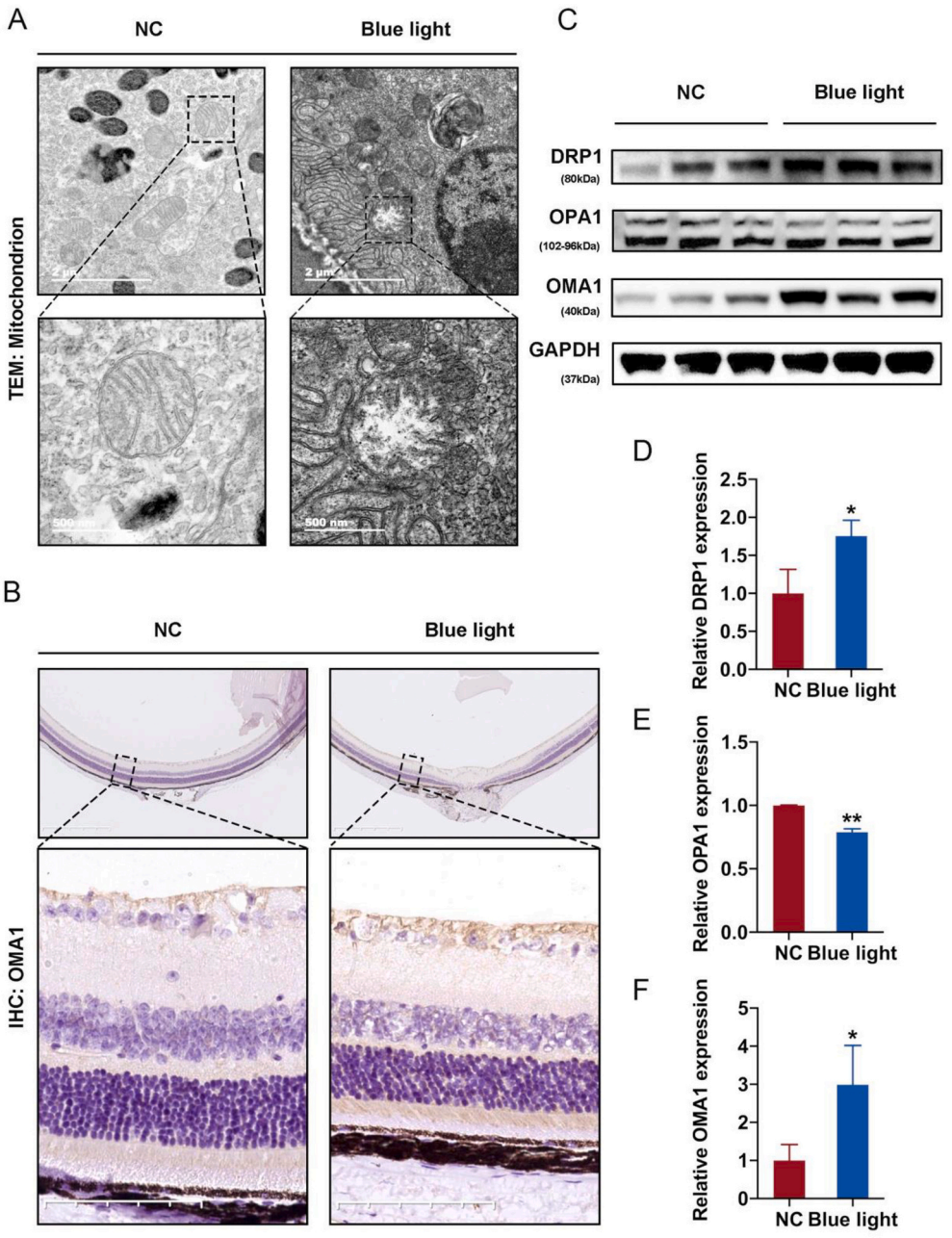

Fig. 2. Alterations in mitochondrial structure- and dynamics-related markers in mice exposed to blue light. (A) TEM revealed a change in the mitochondrial morphology of the mouse RPE in the presence/absence of blue light. (B) The level of OMA1 was validated using immunohistochemical staining. Scale bar = 50 μm. (C) Western blotting assay evaluating the expression of mitochondrial dynamics-associated proteins in mice, including DRP1, OPA1 and OMA1. GAPDH was used as an internal reference. (D—F) The expression levels of DRP1, OPA1 and OMA1 were normalized to those of GAPDH, and the data were recorded as the means ± standard deviations. * $p < 0.05$, ** $p < 0.01$. (For interpretation of the references to colour in this figure legend, the reader is referred to the web version of this article.)

and cell survival [24]. To further study the mechanism underlying retinal injury caused by blue light, it was indispensable to observe the morphology of mitochondria under transmission electron microscopy (TEM). TEM revealed a discrepancy in mitochondria between the groups (Fig. 2A). The TEM images showed a normal structure of mitochondria in normal mouse RPE cells, of which the transverse section was round and the longitudinal section was shoe-shaped, with a clear bilayer membrane and dense mitochondrial cristae formed by orderly arrangement of the inner membrane. In the RPE cells of mice treated with blue light, more mitochondria were destroyed, and the destruction was accompanied by significantly exacerbated vacuolization. After irradiation with blue light, the mitochondrial membranes and cristae appeared to partially to fully disintegrate. The TEM results showed that blue light destroyed the structure of mitochondria in the RPE layer. Mitochondrial structure is coregulated by fusion and fission proteins, and fission is modulated by various proteins, including dynamin-related protein 1 (DRP1) and overlapping activity with m-AAA protease (OMA1), while fusion is controlled by optic atrophy protein 1 (OPA-1) [25,26]. To elucidate the relationship between blue light damage and mitochondrial function, the extracted retinal tissues were analysed for mitochondria-related markers at the protein level. Blue light treatment significantly upregulated DRP1 and OMA1 protein expression and obviously and significantly downregulated OPA1 protein expression (Fig. 2C-F). The same OMA1 expression change was verified by immunohistochemistry, as shown in Fig. 2B: increased immunostaining for OMA1 was observed in blue light–exposed mouse retinas compared with control retinas.

3.3. Cytotoxicity Induced by Blue Light in ARPE-19 Cells

To verify the cytotoxic effect of blue light, we established an ARPE-19 blue light damage model by employing 450 nm blue LED light as the irradiation source. First, ARPE-19 cells were irradiated for various times (6–24 h), and the cell proliferation status was measured by CCK-8 assay. Fig. 3A suggested that blue light damage resulted in a time-dependent reduction in cell viability and that prolongation of the stimulation time exacerbated the decline in cell viability. The ratio of the blue light group to the control group at 12 h was equivalent to that at 24 h, but excessive damage could be avoided with less time. Therefore, 12 h was selected as the stimulation time for subsequent experiments. Tert-butyl hydroperoxide (TBHP) is a widely used trigger of oxidative stress and has been used to induce cellular senescence in multiple kinds of cells [27,28]. To explore blue light-induced retinal cell injury from the perspective of oxidative stress, an oxidative stress model was established as a positive control via the addition of TBHP to the culture medium. The viability of cells treated with different working concentrations of TBHP (50–300 μM) for 12 h was determined by CCK-8 assay to define the final appropriate concentration. Fig. 3B indicated that the toxic effect of TBHP on ARPE-19 cells was concentration dependent. The effective concentration of 100 μM induced an effect similar to that of blue light exposure, and 100 μM TBHP was used to establish a positive control. Flow cytometry analysis with FITC-Annexin V and PI colabelling demonstrated that, similar to the positive control treatment, blue light exposure for 12 h induced an approximately 2.9-fold increase in apoptotic cells (Q2 + Q3), of which late apoptotic cells (Q2) composed the majority (Fig. 3 C—D). The results showed that blue light irradiation for 12 h induced ARPE-19 apoptosis in a manner similar to oxidative stress with late apoptosis.

3.4. ROS Generation in ARPE-19 Cells Exposed to Blue Light

Furthermore, total ROS generation was analysed after 12 h by both flow cytometry and immunofluorescence assays. As expected, irradiation with blue light increased the general ROS levels, as reflected by the flow cytometry results (Fig. 4A-B). Similarly, FITC-labelled DCFH-DA-stained ARPE-19 cells were examined under a fluorescence microscope, and as shown in Fig. 4C-D, the fluorescence intensity in the positive control group and blue light group was significantly higher than that in

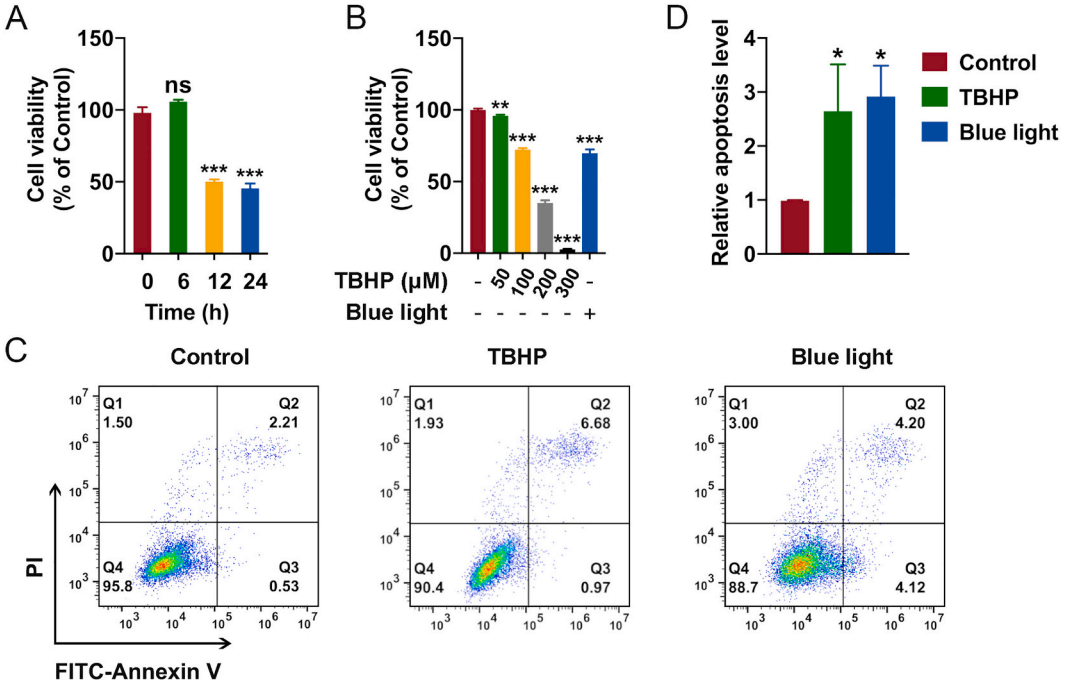

Fig. 3. Blue light and TBHP reduced cell viability and induced apoptosis in ARPE-19 cells. (A) Assessment of cell viability and death after exposure of ARPE-19 cells to blue light for multiple durations from 6 to 24 h by CCK-8 assay. (B) Treatment with 0 μM, 50 μM, 100 μM, 200 μM, or 300 μM TBHP for 12 h reduced cell viability in a concentration-dependent manner, as detected by CCK-8 assay. (C) Apoptosis in ARPE-19 cells caused by TBHP treatment or blue light exposure was determined using PI and Annexin V-FITC double staining and flow cytometry. (D) Quantitative results of total apoptosis as determined by flow cytometry in the control group, TBHP group and blue light group. * $p < 0.05$, ** $p < 0.01$, *** $p < 0.001$. (For interpretation of the references to colour in this figure legend, the reader is referred to the web version of this article.)

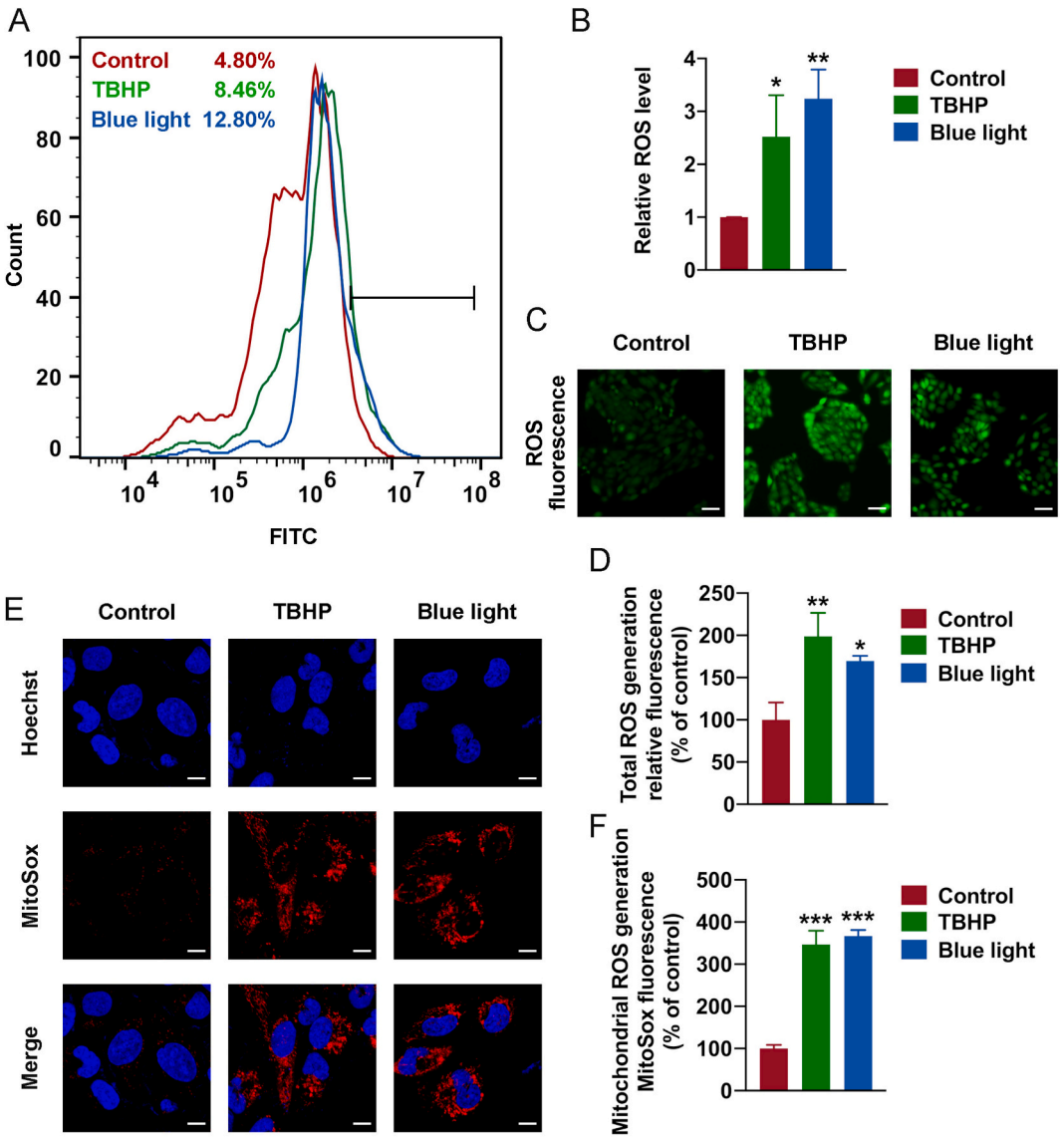

Fig. 4. Blue light triggered increases in ROS levels in vitro. ARPE-19 cells were treated with 100 μM TBHP or blue light for 12 h. Total ROS production was measured by (A) flow cytometry and (C) immunofluorescence; scale bar = 100 μm. (B) Quantitative results of total ROS generation as analysed by flow cytometry using CM-H2DCFDA labelling. (D) Quantitative results of relative ROS generation as measured by immunofluorescence using DCFH-DA staining. (E) Representative micrographs of MitoSox Red-labelled ARPE-19 cells in the control group and in the presence of 100 μM TBHP or blue light for 12 h. Red: MitoSox Red, blue: nuclei stained with Hoechst. Scale bar = 30 μm. (F) Scale of the relative fluorescence intensities of MitoSox Red in the other two groups compared to the control group. * $p < 0.05$, ** $p < 0.01$, *** $p < 0.001$. (For interpretation of the references to colour in this figure legend, the reader is referred to the web version of this article.)

the control group. Quantitative analysis of the relative fluorescence strength with Image J software revealed that the fluorescence intensity of ROS in the blue light irradiation group was 1.7-fold higher than that in the negative control group, while a 2-fold increase was observed in the TBHP group. Then, we stained ARPE-19 cells with the probe MitoSox Red to verify whether the source of ROS was related to mitochondria. Remarkably, the results obtained with TBHP and blue light stimulation were similar, suggesting that ROS produced by mitochondria were specifically detected. We used the highly selective fluorescent dye MitoSox Red to gauge mitochondria-derived ROS and discovered via confocal fluorescence microscopy that the fluorescence intensity of MitoSox Red was significantly enhanced in ARPE-19 cells treated with TBHP or blue light (Fig. 4E-F). This finding suggested that blue light strongly induced ROS production within the mitochondria of ARPE-19 cells through oxidative stress.

3.5. Mitochondrial Dynamics Damage Caused by Light-Induced Oxidative Stress

Mitochondrial morphology is quite dynamic even under physiological conditions, and mitochondria tend to fragment under exposure to various stressors. Light-induced mitochondrial fragmentation has also been reported by numerous studies [16,19,20]. Therefore, the mitochondrial morphology in ARPE-19 cells was characterized using the Mito-Tracker Green probe. The mitochondria in the control group presented a network structure, while TBHP and blue light treatment promoted mitochondrial fragmentation. Additionally, the mitochondria were altered to uniformly punctate organelles, indicating that oxidative stress and blue light exposure substantially disrupted the mitochondrial morphology in ARPE-19 cells (Fig. 5A-B). Then we assayed the protein levels of mitochondrial dynamics-related proteins (OMA1, OPA1 and DRP1) by immunoblotting. In human cells, OPA1, the activator of mitochondrial membrane merging, has been reported to exist in five

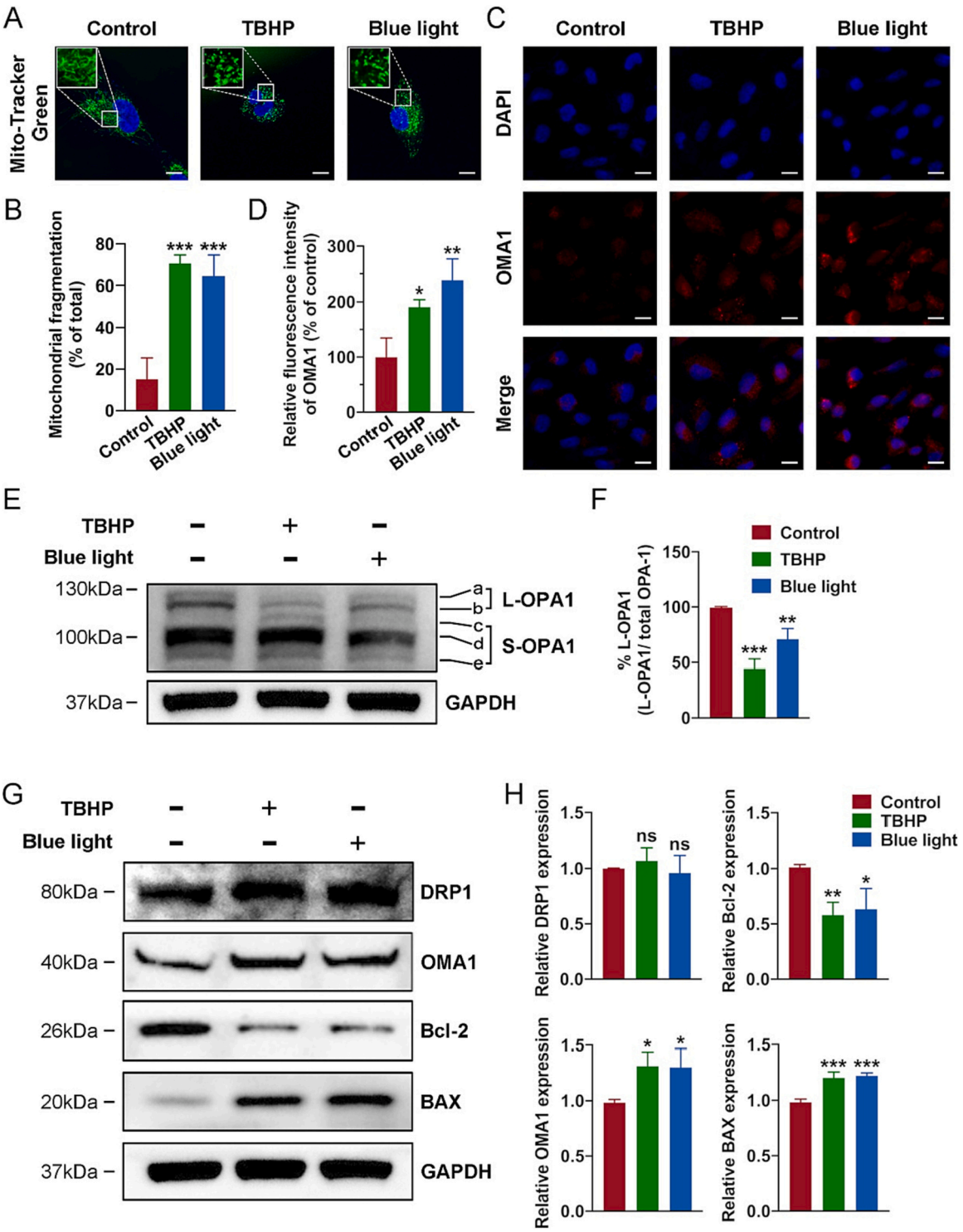

Fig. 5. Mitochondrial dynamics were destroyed by blue light in ARPE-19 cells. ARPE-19 cells were treated with 100 μM TBHP or blue light for 12 h. (A) Representative micrographs of MitoTracker-labelled ARPE-19 cells in the control group and those exposed to 100 μM TBHP or blue light for 12 h. Green: MitoTracker, blue: nuclei stained with Hoechst. Scale bar = 30 μm. The upper left panel shows a high-magnification image corresponding to the indicated region in the original image. (B) Quantitative results of ratio of the mitochondrial fragmentation among the control group, TBHP group and blue light group. (C) Representative images of OMA1 expression as tested by immunofluorescence. Scale bar = 20 μm. (D) Quantitative results of the relative fluorescence intensities among the control group, TBHP group and blue light group. (E) Anti-OPA1 western blotting of ARPE-19 cells. The positions of the L-OPA1 (a, b) and S-OPA1 (c–e) isoforms are labelled as indicated. (F) The expression level of L-OPA1 was normalized to that of GAPDH and quantified. (G) Western blotting assay evaluating the expression of mitochondrial dynamics-associated proteins, including DRP1 and OMA1, and mitochondrial apoptosis-associated proteins, including Bcl-2 and BAX. GAPDH was used as an internal reference. (H) The expression levels of DRP1, OMA1, Bcl-2 and BAX were normalized to those of GAPDH. * $p < 0.05$, ** $p < 0.01$, *** $p < 0.001$. (For interpretation of the references to colour in this figure legend, the reader is referred to the web version of this article.)

isoforms. The two longer isoforms (a and b) are defined as L-OPA1 and contribute to mitochondrial inner membrane fusion, while the three shorter and nonfunctional isoforms (c, d, and e) are defined as S-OPA1 [29,30]. OMA1 partially mediates the conversion of L-OPA1 to S-OPA1 [31]. Consistent with previous studies, upon blue light insult, OMA1 expression significantly increased, while the percentage of L-OPA1 expression within total OPA1 protein expression decreased, disrupting mitochondrial fusion. However, DRP1 protein expression remained unchanged (Fig. 5E-H). Moreover, immunostaining indicated that OMA1 was activated and its expression was increased in the positive control group and the blue light group (Fig. 5C-D). Western blotting assays showed that mitochondrial apoptosis-associated proteins were affected as well. The group treated with blue light exhibited a decrease in the Bcl-2 protein level and an increase in the Bax protein level (Fig. 5G-H). Taken together, these results sugged that blue light damaged mitochondrial dynamics by mainly activating OMA1 to cleave L-OPA1 to reduce mitochondrial fusion but did not change the expression of DRP1 and induced mitochondria-mediated apoptosis in ARPE-19 cells.

4. Discussion

The incidence of AMD has been found to be related to environmental and genetic factors [4,32]. Although the aggravating influence of blue light on retinal degeneration has been reported [33], the RPE cell damage induced by blue light has not been fully elucidated. In this study, we investigated the mitochondrial dynamics alterations that occur in the context of blue LED light-induced retinal degeneration and oxidative injury in mouse retinal tissues and ARPE-19 cells. Our findings revealed that exposure to blue light excessively induced OMA1 expression to disrupt the balance of mitochondrial dynamics and promote mitochondrial fragmentation, which resulted in excessive oxidative stress and eventually led to retinal cell death.

The findings in this research showed that exposure of 6-month-old mice to 800 lx of blue LED light for two weeks damaged retinal tissue. HE and TUNEL staining data demonstrated that long-term irradiation with blue light led to apoptosis and cell death, especially in the ONL and RPE (Fig. 1). Microstructural features, including mitochondrial fragmentation, vacuolization, mitochondrial cristae rarefaction and destruction, were observed under TEM, suggesting that blue LED light disrupted the balance of mitochondrial homeostasis and destroyed mitochondrial structure. These outcomes were verified by the results of western blotting of structure-related mitochondrial proteins purified from mouse retinas (Fig. 2). However, no severe retinal damage appeared in the mice in the negative control group. There are a few causes of this difference. Blue light, mainly blue light with a wavelength of 415–460 nm, is regarded as the source of 80% of damage to the retina [16]. This is why the main wavelength of the light applied in this study was 450 nm with a half bandwidth at 15 nm, which almost covered the most harmful frequency band. Previous studies have demonstrated that exposure to blue light at certain doses induces intracellular oxidative stress and ROS aggregation in mitochondria, causing cell death [34,35]. It has also been reported that overproduced ROS target cellular compartments such as mitochondria and activate mitochondria-dependent apoptosis [36,37]. Considering that structural deficiency of mitochondria is a main characteristic of mitochondrial disorder that may be strongly connected with mitochondria-dependent apoptosis [38,39], we speculated that blue light-induced retinal injury is inseparable from changes in mitochondrial proteins. This speculation was verified by observation of the morphology of mitochondria in the RPE by TEM and examination of the expression of mitochondrial structure-related proteins, including DRP1, OMA1, and OPA1. Consistently, OPA1, the typical mitochondrial fusion-regulating protein, was downregulated in mouse total retinas after treatment with blue light, while DRP1 and OMA1 appeared to be upregulated to promote mitochondrial fission. Notably, the proteins examined by western blotting were extracted from the whole retinal tissue, which contained not only RPE cells but also PR cells, bipolar cells, and retinal ganglion cells. RPE cells are critical for maintaining the physiological status of the choriocapillaris and PRs, so degeneration of RPE cells is considered to be a characteristic of dry AMD [40,41]. In addition, RPE cells are relatively sensitive to blue light [15]. Therefore, research on the pathogenesis of AMD mainly focuses on the RPE [42–45], and the current study chose ARPE-19 cells in vitro to further investigate the underlying mitochondrial changes.

The in vitro experiments also yielded several findings. First, blue light caused time-dependent damage to ARPE-19 cells, consistent with the results of previous studies [46–48]. Similar to the direct TBHP-mediated induction of oxidative stress, long-term irradiation with blue light for 12 h induced significant apoptosis and marked ROS production, which implied that blue light exerted a cytotoxic influence on ARPE-19 cells by inducing intracellular oxidative stress (Fig. 3). We specifically detected ROS generated in mitochondria using selective probes and found that blue light exposure induced excessive ROS production in dysfunctional mitochondria (Fig. 4). Interestingly, when we focused on mitochondria-shaping markers that affect mitochondrial function, we found that DRP1 levels did not differ among the negative control group, positive control group and blue light-exposed group, in contrast to the results in vivo. The OPA1 protein has five isoforms in human cells but only two isoforms in mouse cells, which explains the difference in the western blotting images between the in vivo and in vitro models. In ARPE-19 cells, the increase in OMA1 expression upon blue light insult aggravated the cleavage and inactivation of L-OPA1, further blocking fusion in mitochondria [31]. This imbalance in mitochondrial fusion–fission dynamics markers implied that under long-term blue light irradiation, a decrease in fusion impaired the function of mitochondria to a greater extent than promotion of fission in ARPE-19 cells (Fig. 5). Previous evidence indicates that OMA1 plays a critical role in stabilizing the mitochondrial inner membrane to block cytochrome *c*, the key regulator of apoptosis, inside cristae and prevent its release into the cytoplasm [49–52]. These findings suggest that the destruction of the mitochondrial inner membrane may be associated with the development of blue light-induced retinal degeneration and that the interaction between OPA1 and OMA1 may play an important role.

Notably, earlier blue light-damage models were often based on BALB/c mice [53], ddY mice [54], albino Hds/Win333:NMRI mice [55]. For example, GH Kim et al. explored phenotypes of light-emitting diode-induced retinal degeneration in BALB/c mice [56]. The animals mentioned above lack melanosomes. However, melanosomes are present in the RPE in human eyes, and they play important roles in light absorption and removing free radicals from the RPE [40]. Because C57BL/6 mice have melanosomes, the animal model in the current study provides a better indication of the light-induced damage to the human retina from the perspective of retinal structure. The International Commission on Non-Ionizing Radiation Protection proposed a guideline: 110 kJ/m2 has been evaluated as the toxic dose of blue light from ocular instruments that can induce macroscopically observable retinal lesions [11]. Therefore, the present experiment exposed mice to blue light at an illuminance of 800 lx for 14 days in 12-h periods of dark and light. The cumulative dose of blue light to which mice were exposed was equal to that recommended in the guideline. Compared to earlier studies [56,57], we reset the illuminance and duration of light treatment based on the guideline described above, and the purpose of the current study was to establish a light-induced retinal damage model and to explore the mechanism and pathophysiological characteristics of this model. Pathological changes in the retina, including the RPE layer, caused by exposure to blue LED light have been characterized in a similar model [57]. However, the alterations in mitochondrial morphology and the definite discrepancies in the expression of proteins related to the regulation of mitochondrial structure induced by short wavelength light exposure were first clarified in vivo in the current study. This work originally reported TEM results for mitochondrial destruction in the RPE layer of pigmented mice upon long-term blue LED light exposure and

first detected markers of mitochondrial dynamics in vivo, revealing the obstruction of mitochondrial dynamics at the levels of histology and molecular biology.

Although this study has addressed the impacts of blue light on dynamics of mitochondria in vivo and in vitro, several limitations also apply. One limitation was the equipment. This study only assessed retinal degeneration in vivo from the perspective of anatomy and molecular biology. If possible, observations of both functional and morphological changes using electroretinograms (ERG) and spectral domain-OCT are valuable. Above exams would help to determine the performance of AMD. Secondly, additional tests involving overexpression of OPA1 or knockdown of OMA1 should be performed to verify the association between OPA1 and OMA1 and blue light-induced retinal damage. Moreover, the intensity and duration of blue LED light exposure seems a little excessive for mice. Thus, researchers would carefully consider further optimizing the light-induced damage model in mice, for example by decreasing the light power and maintaining the same light dose, to better reflect the effects on human eyes in subsequent experiments.

In conclusion, long-term exposure to blue light resulted in damage to the retina in mice, particularly the ONL and RPE cells. Mitochondrial destruction and dysfunction were observed in RPE cells in vivo and in vitro. Mitochondrial dynamics were disrupted with characteristics of fusion-related obstruction after blue light irradiation. These findings might help improve blue light-induced retinal degeneration models in vivo and thoroughly investigate the pathogenesis of AMD.

Financial Support

This work was supported by the Strategic Priority Research Program of Chinese Academy of Sciences (Grant Number XDA16040200), the National Natural Science Foundation of China (Grant Number 8220040041), the Natural Science Foundation of Zhejiang Province (Grant Number LZ19H120001), the Major Science and Technology Project of Zhejiang Province (Grant Number 2018C03017), the Science Foundation of National Health and Family Planning Commission (Grant Number 2018273457), the National Natural Science Foundation of China (Grant Number 81800868), the Health and Family Planning Commission of Zhejiang Province, China (Grant Number 2018KY057).

CRediT authorship contribution statement

Liyin Wang: Conceptualization, Methodology, Writing – original draft. **Xin Yu:** Conceptualization, Methodology, Writing – original draft. **Dongyan Zhang:** Conceptualization, Methodology, Writing – original draft. **Yingying Wen:** Methodology, Software, Investigation. **Liyue Zhang:** Investigation, Data curation. **Yutong Xia:** Investigation, Visualization, Writing – review & editing. **Jinbo Chen:** Visualization, Writing – review & editing. **Chen Xie:** Supervision, Funding acquisition. **Hong Zhu:** Visualization, Writing – review & editing. **Jianping Tong:** Conceptualization, Methodology, Formal analysis, Writing – review & editing, Project administration, Visualization. **Ye Shen:** Conceptualization, Methodology, Formal analysis, Writing – review & editing, Project administration, Visualization.

Declaration of Competing Interest

The authors declare that there are no conflicts of interest.
No conflicting relationship exists for any author.

Data availability

Data will be made available on request.

References

[1] R. Kawasaki, M. Yasuda, S.J. Song, S.J. Chen, J.B. Jonas, J.J. Wang, P. Mitchell, T. Y. Wong, The prevalence of age-related macular degeneration in Asians: a systematic review and meta-analysis, Ophthalmology 117 (5) (2010) 921–927.
[2] W.L. Wong, X. Su, X. Li, C.M.G. Cheung, R. Klein, C.-Y. Cheng, T.Y. Wong, Global prevalence of age-related macular degeneration and disease burden projection for 2020 and 2040: a systematic review and meta-analysis, Lancet Glob. Health 2 (2) (2014) e106–e116.
[3] W. Tan, J. Zou, S. Yoshida, B. Jiang, Y. Zhou, The role of inflammation in age-related macular degeneration, Int. J. Biol. Sci. 16 (15) (2020) 2989–3001.
[4] P. Mitchell, G. Liew, B. Gopinath, T.Y. Wong, Age-related macular degeneration, Lancet 392 (10153) (2018) 1147–1159.
[5] Z. Hu, X. Lv, L. Chen, X. Gu, H. Qian, S. Fransisca, Z. Zhang, Q. Liu, P. Xie, Protective effects of microRNA-22-3p against retinal pigment epithelial inflammatory damage by targeting NLRP3 inflammasome, J. Cell. Physiol. 234 (10) (2019) 18849–18857.
[6] V.M. Villegas, L.A. Aranguren, J.L. Kovach, S.G. Schwartz, H.W. Flynn Jr., Current advances in the treatment of neovascular age-related macular degeneration, Expert. Opin. Drug Deliv. 14 (2) (2017) 273–282.
[7] S. Datta, M. Cano, K. Ebrahimi, L. Wang, J.T. Handa, The impact of oxidative stress and inflammation on RPE degeneration in non-neovascular AMD, Prog. Retin. Eye Res. 60 (2017) 201–218.
[8] S.K. Mitter, C. Song, X. Qi, H. Mao, H. Rao, D. Akin, A. Lewin, M. Grant, W. Dunn Jr., J. Ding, C. Bowes Rickman, M. Boulton, Dysregulated autophagy in the RPE is associated with increased susceptibility to oxidative stress and AMD, Autophagy 10 (11) (2014) 1989–2005.
[9] J. Hanus, C. Anderson, S. Wang, RPE necroptosis in response to oxidative stress and in AMD, Ageing Res. Rev. 24 (Pt B) (2015) 286–298.
[10] M.A. Mainster, Violet and blue light blocking intraocular lenses: photoprotection versus photoreception, Br. J. Ophthalmol. 90 (6) (2006) 784–792.
[11] I.C.o.N.-I.R. Protection, Guidelines on Limits of Exposure to Incoherent Visible and Infrared Radiation, International Commission on Non-Ionizing Radiation Protection, Health Phys, 2013.
[12] E.K. Ozkaya, G. Anderson, B. Dhillon, P.O. Bagnaninchi, Blue-light induced breakdown of barrier function on human retinal epithelial cells is mediated by PKC-zeta over-activation and oxidative stress, Exp. Eye Res. 189 (2019), 107817.
[13] T. Kurihara, M. Omoto, K. Noda, M. Ebinuma, S. Kubota, H. Koizumi, S. Yoshida, Y. Ozawa, S. Shimmura, S. Ishida, K. Tsubota, Retinal phototoxicity in a novel murine model of intraocular lens implantation, Mol. Vis. 15 (2009) 2751–2761.
[14] N. Vila, A. Siblini, E. Esposito, V. Bravo-Filho, P. Zoroquiain, S. Aldrees, P. Logan, L. Arias, M.N. Burnier, Blue-light filtering alters angiogenic signaling in human retinal pigmented epithelial cells culture model, BMC Ophthalmol. 17 (1) (2017) 198.
[15] P.V. Algvere, J. Marshall, S. Seregard, Age-related maculopathy and the impact of blue light hazard, Acta Ophthalmol. Scand. 84 (1) (2006) 4–15.
[16] X. Liu, Q. Zhou, H. Lin, J. Wu, Z. Wu, S. Qu, Y. Bi, The protective effects of blue light-blocking films with different shielding rates: a rat model study, Transl. Vis. Sci. Technol. 8 (3) (2019) 19.
[17] S.G. Jarrett, H. Lin, B.F. Godley, M.E. Boulton, Mitochondrial DNA damage and its potential role in retinal degeneration, Prog. Retin. Eye Res. 27 (6) (2008) 596–607.
[18] F.-Q. Liang, B.F. Godley, Oxidative stress-induced mitochondrial DNA damage in human retinal pigment epithelial cells: a possible mechanism for RPE aging and age-related macular degeneration, Exp. Eye Res. 76 (4) (2003) 397–403.
[19] Y. Yang, S. Karakhanova, W. Hartwig, J.G. D'Haese, P.P. Philippov, J. Werner, A. V. Bazhin, Mitochondria and mitochondrial ROS in Cancer: novel targets for anticancer therapy, J. Cell. Physiol. 231 (12) (2016) 2570–2581.
[20] H. Chen, D.C. Chan, Emerging functions of mammalian mitochondrial fusion and fission, Hum. Mol. Genet. 14 (2005). Spec no2. R283–9.
[21] B. Westermann, Bioenergetic role of mitochondrial fusion and fission, Biochim. Biophys. Acta 1817 (10) (2012) 1833–1838.
[22] K.C. Chuang, C.R. Chang, S.H. Chang, S.W. Huang, S.M. Chuang, Z.Y. Li, S. T. Wang, J.K. Kao, Y.J. Chen, J.J. Shieh, Imiquimod-induced ROS production disrupts the balance of mitochondrial dynamics and increases mitophagy in skin cancer cells, J. Dermatol. Sci. 98 (3) (2020) 152–162.
[23] B. Chen, H. Li, G. Ou, L. Ren, X. Yang, M. Zeng, Curcumin attenuates MSU crystal-induced inflammation by inhibiting the degradation of IkappaBalpha and blocking mitochondrial damage, Arthritis Res. Ther. 21 (1) (2019) 193.
[24] F.J. Bock, S.W.G. Tait, Mitochondria as multifaceted regulators of cell death, Nat. Rev. Mol. Cell Biol. 21 (2) (2020) 85–100.
[25] S. Rovira-Llopis, C. Banuls, N. Diaz-Morales, A. Hernandez-Mijares, M. Rocha, V. M. Victor, Mitochondrial dynamics in type 2 diabetes: pathophysiological implications, Redox Biol. 11 (2017) 637–645.
[26] A.M. van der Bliek, Q. Shen, S. Kawajiri, Mechanisms of mitochondrial fission and fusion, Cold Spring Harb. Perspect. Biol. 5 (6) (2013).
[27] O. Kucera, R. Endlicher, T. Rousar, H. Lotkova, T. Garnol, Z. Drahota, Z. Cervinkova, The effect of tert-butyl hydroperoxide-induced oxidative stress on lean and steatotic rat hepatocytes in vitro, Oxidative Med. Cell. Longev. 2014 (2014), 752506.
[28] S. Wedel, I. Martic, N. Hrapovic, S. Fabre, C.T. Madreiter-Sokolowski, T. Haller, G. Pierer, C. Ploner, P. Jansen-Durr, M. Cavinato, tBHP treatment as a model for cellular senescence and pollution-induced skin aging, Mech. Ageing Dev. 190 (2020), 111318.
[29] L. Griparic, T. Kanazawa, A.M. van der Bliek, Regulation of the mitochondrial dynamin-like protein Opa1 by proteolytic cleavage, J. Cell Biol. 178 (5) (2007) 757–764.

[30] E. Jones, N. Gaytan, I. Garcia, A. Herrera, M. Ramos, D. Agarwala, M. Rana, W. Innis-Whitehouse, E. Schuenzel, R. Gilkerson, A threshold of transmembrane potential is required for mitochondrial dynamic balance mediated by DRP1 and OMA1, Cell. Mol. Life Sci. 74 (7) (2017) 1347–1363.
[31] S. Ehses, I. Raschke, G. Mancuso, A. Bernacchia, S. Geimer, D. Tondera, J. C. Martinou, B. Westermann, E.I. Rugarli, T. Langer, Regulation of OPA1 processing and mitochondrial fusion by m-AAA protease isoenzymes and OMA1, J. Cell Biol. 187 (7) (2009) 1023–1036.
[32] M. Fleckenstein, T.D.L. Keenan, R.H. Guymer, U. Chakravarthy, S. Schmitz-Valckenberg, C.C. Klaver, W.T. Wong, E.Y. Chew, Age-related macular degeneration, Nat. Rev. Dis. Primers 7 (1) (2021) 31.
[33] W. Hao, A. Wenzel, M.S. Obin, C.K. Chen, E. Brill, N.V. Krasnoperova, P. Eversole-Cire, Y. Kleyner, A. Taylor, M.I. Simon, C. Grimm, C.E. Reme, J. Lem, Evidence for two apoptotic pathways in light-induced retinal degeneration, Nat. Genet. 32 (2) (2002) 254–260.
[34] B. Pavan, A. Dalpiaz, Retinal pigment epithelial cells as a therapeutic tool and target against retinopathies, Drug Discov. Today 23 (9) (2018) 1672–1679.
[35] A. King, E. Gottlieb, D.G. Brooks, M.P. Murphy, J.L. Dunaief, Mitochondria-derived reactive oxygen species mediate blue light-induced death of retinal pigment epithelial cells, Photochem. Photobiol. 79 (5) (2004) 470–475.
[36] N. Ueda, Ceramide-induced apoptosis in renal tubular cells: a role of mitochondria and sphingosine-1-phoshate, Int. J. Mol. Sci. 16 (3) (2015) 5076–5124.
[37] C. Huang, P. Zhang, W. Wang, Y. Xu, M. Wang, X. Chen, X. Dong, Long-term blue light exposure induces RGC-5 cell death in vitro: involvement of mitochondria-dependent apoptosis, oxidative stress, and MAPK signaling pathways, Apoptosis 19 (6) (2014) 922–932.
[38] U. Paasch, S. Grunewald, S. Dathe, H.J. Glander, Mitochondria of human spermatozoa are preferentially susceptible to apoptosis, Ann. N. Y. Acad. Sci. 1030 (2004) 403–409.
[39] A. Amaral, B. Lourenco, M. Marques, J. Ramalho-Santos, Mitochondria functionality and sperm quality, Reproduction 146 (5) (2013) R163–R174.
[40] O. Strauss, The retinal pigment epithelium in visual function, Physiol. Rev. 85 (3) (2005) 845–881.
[41] H. Kokotas, M. Grigoriadou, M.B. Petersen, Age-related macular degeneration: genetic and clinical findings, Clin. Chem. Lab. Med. 49 (4) (2011) 601–616.
[42] M. Zou, Q. Ke, Q. Nie, R. Qi, X. Zhu, W. Liu, X. Hu, Q. Sun, J.L. Fu, X. Tang, Y. Liu, D.W. Li, L. Gong, Inhibition of cGAS-STING by JQ1 alleviates oxidative stress-induced retina inflammation and degeneration, Cell Death Differ 29 (9) (2022) 1816–1833.
[43] J.Z. Chuang, N. Yang, N. Nakajima, W. Otsu, C. Fu, H.H. Yang, M.P. Lee, A. F. Akbar, T.C. Badea, Z. Guo, A. Nuruzzaman, K.S. Hsu, J.L. Dunaief, C.H. Sung, Retinal pigment epithelium-specific CLIC4 mutant is a mouse model of dry age-related macular degeneration, Nat. Commun. 13 (1) (2022) 374.
[44] K.V. Manian, C.A. Galloway, S. Dalvi, A.A. Emanuel, J.A. Mereness, W. Black, L. Winschel, C. Soto, Y. Li, Y. Song, W. DeMaria, A. Kumar, I. Slukvin, M. P. Schwartz, W.L. Murphy, B. Anand-Apte, M. Chung, D.S.W. Benoit, R. Singh, 3D iPSC modeling of the retinal pigment epithelium-choriocapillaris complex identifies factors involved in the pathology of macular degeneration, Cell Stem Cell 28 (5) (2021) 846–862.e8.
[45] L. da Cruz, K. Fynes, O. Georgiadis, J. Kerby, Y.H. Luo, A. Ahmado, A. Vernon, J. T. Daniels, B. Nommiste, S.M. Hasan, S.B. Gooljar, A.F. Carr, A. Vugler, C. M. Ramsden, M. Bictash, M. Fenster, J. Steer, T. Harbinson, A. Wilbrey, A. Tufail, G. Feng, M. Whitlock, A.G. Robson, G.E. Holder, M.S. Sagoo, P.T. Loudon, P. Whiting, P.J. Coffey, Phase 1 clinical study of an embryonic stem cell-derived retinal pigment epithelium patch in age-related macular degeneration, Nat. Biotechnol. 36 (4) (2018) 328–337.
[46] K.C. Cheng, Y.T. Hsu, W. Liu, H.L. Huang, L.Y. Chen, C.X. He, S.J. Sheu, K.J. Chen, P.Y. Lee, Y.H. Lin, C.C. Chiu, The role of oxidative stress and autophagy in blue-light-induced damage to the retinal pigment epithelium in zebrafish in vitro and in vivo, Int. J. Mol. Sci. 22 (3) (2021).
[47] K. Takayama, H. Kaneko, K. Kataoka, R. Kimoto, S.J. Hwang, F. Ye, Y. Nagasaka, T. Tsunekawa, T. Matsuura, N. Nonobe, Y. Ito, H. Terasaki, Nuclear factor (erythroid-derived)-related factor 2-associated retinal pigment epithelial cell protection under blue light-induced oxidative stress, Oxidative Med. Cell. Longev. 2016 (2016) 8694641.
[48] H.Y. Youn, V. Bantseev, N.C. Bols, A.P. Cullen, J.G. Sivak, In vitro assays for evaluating the ultraviolet B-induced damage in cultured human retinal pigment epithelial cells, J. Photochem. Photobiol. B 88 (1) (2007) 21–28.
[49] C. Frezza, S. Cipolat, O. Martins de Brito, M. Micaroni, G.V. Beznoussenko, T. Rudka, D. Bartoli, R.S. Polishuck, N.N. Danial, B. De Strooper, L. Scorrano, OPA1 controls apoptotic cristae remodeling independently from mitochondrial fusion, Cell 126 (1) (2006) 177–189.
[50] X. Liu, C.N. Kim, J. Yang, R. Jemmerson, X. Wang, Induction of apoptotic program in cell-free extracts: requirement for dATP and cytochrome c, Cell 86 (1) (1996) 147–157.
[51] A. Olichon, L. Baricault, N. Gas, E. Guillou, A. Valette, P. Belenguer, G. Lenaers, Loss of OPA1 perturbates the mitochondrial inner membrane structure and integrity, leading to cytochrome c release and apoptosis, J. Biol. Chem. 278 (10) (2003) 7743–7746.
[52] S. Cipolat, T. Rudka, D. Hartmann, V. Costa, L. Serneels, K. Craessaerts, K. Metzger, C. Frezza, W. Annaert, L. D'Adamio, C. Derks, T. Dejaegere, L. Pellegrini, R. D'Hooge, L. Scorrano, B. De Strooper, Mitochondrial rhomboid PARL regulates cytochrome c release during apoptosis via OPA1-dependent cristae remodeling, Cell 126 (1) (2006) 163–175.
[53] B.L. Lee, J.H. Kang, H.M. Kim, S.H. Jeong, D.S. Jang, Y.P. Jang, S.Y. Choung, Polyphenol-enriched Vaccinium uliginosum L. fractions reduce retinal damage induced by blue light in A2E-laden ARPE19 cell cultures and mice, Nutr. Res. 36 (12) (2016) 1402–1414.
[54] M. Nakamura, Y. Kuse, K. Tsuruma, M. Shimazawa, H. Hara, The involvement of the oxidative stress in murine blue LED light-induced retinal damage model, Biol. Pharm. Bull. 40 (8) (2017) 1219–1225.
[55] J. Vicente-Tejedor, M. Marchena, L. Ramirez, D. Garcia-Ayuso, V. Gomez-Vicente, C. Sanchez-Ramos, P. de la Villa, F. Germain, Removal of the blue component of light significantly decreases retinal damage after high intensity exposure, PLoS One 13 (3) (2018), e0194218.
[56] G.H. Kim, H.I. Kim, S.S. Paik, S.W. Jung, S. Kang, I.B. Kim, Functional and morphological evaluation of blue light-emitting diode-induced retinal degeneration in mice, Graefes Arch. Clin. Exp. Ophthalmol. 254 (4) (2016) 705–716.
[57] M. Nakamura, T. Yako, Y. Kuse, Y. Inoue, A. Nishinaka, S. Nakamura, M. Shimazawa, H. Hara, Exposure to excessive blue LED light damages retinal pigment epithelium and photoreceptors of pigmented mice, Exp. Eye Res. 177 (2018) 1–11.